16TH EUROPEAN CONFERENCE ON EARTHQUAKE ENGINEERING THESSALONIKI 18 - 21 JUNE 2018

Nonlinear Analysis of Square CFT Columns with Fiber Beam/Column Element

Nikola BLAGOJEVIĆ[1], Svetlana M. KOSTIĆ[2]

ABSTRACT

The use of concrete filled steel tubes (CFT columns) in seismically active regions is becoming more common and widespread due to numerous advantages they offer over steel and reinforced concrete columns, such as increased ductility, buckling delay and good cyclic performance. Since the behavior of CFT columns is highly nonlinear, a numerical model needs to consider different nonlinear effects. The model proposed in this paper adopts the nonlinear force based beam/column element that takes into account the nonlinear behavior of steel and concrete, confinement effects and geometrical nonlinearities. Through a parametric study, different material models for steel and concrete, widely available in commercial software programs, are evaluated and the constitutive model parameters that best approximate the behavior of CFT columns under static loading conditions are determined. This numerical model is then validated through a comparison with a number of experimental tests from the literature. Different types of loading (cyclic static and dynamic), types of structures with different slenderness of tested specimens and B/t ratio are considered. In addition, limitations of the proposed fiber element model for modelling CFT columns are emphasized.

Keywords: composite columns; distributed plasticity; numerical analysis; uniaxial material model; OpenSEES

1. INTRODUCTION

Concrete filled steel tubes (CFT columns) are in increasing use in contemporary engineering practice since they offer a number of advantages over steel and reinforced concrete members, such as higher strength, increased ductility, buckling delay or prevention, better fire performances, etc. Their behavior is highly nonlinear due to nonlinear constituent materials, steel and concrete, buckling of the steel tube and slip at the steel-concrete interface. Therefore, in order to perform a reliable numerical analysis, an adequate nonlinear model is required. Up to date, numerous nonlinear models for modelling CFT columns exist. Among them, most widely used are fiber based beam/column models that have shown to be computationally very efficient and with a high level of accuracy (Tort and Hajjar 2009; Valipour and Foster 2010).

The accuracy of the fiber based beam/column elements strongly depends on the constitutive material models for steel and concrete assigned to the steel and concrete fibers of the cross-section. In the last decade, several material models are proposed specifically for analysis of CFT columns (Portolés et al. 2011; M. D. Denavit, Hajjar, and Leon 2012; Valipour and Foster 2010; Varma et al. 2005). However, most of them are not implemented in analysis software packages yet and are not easily accessible. Therefore, in the study presented in this paper, the distributed plasticity force based beam/column element by Taucer, Spacone and Filippou (1991) together with the constitutive material models for steel and concrete available in OpenSEES (McKenna, Frank, G. L. Fenves and M. H. Scott 2000) and most other nonlinear analysis software packages, are evaluated in nonlinear analysis of square CFT columns. This paper presents the results of the parameter study and proposes the material model parameters that offer the best correlation with the experimental tests available in the literature.

[1]Teaching assistant/PhD Student, MSc, Belgrade, Serbia, nblagojevic@grf.bg.ac.rs
[2]Assistant Professor, PhD, Belgrade, Serbia, svetlana@grf.bg.ac.rs

2. MATERIAL MODELS

In order to evaluate different material models for steel and concrete in nonlinear analysis of CFT columns, the parametric study is conducted (Blagojević 2016). Results of this study are presented below.
All numerical simulations are performed in OpenSEES (McKenna, Frank, G. L. Fenves and M. H. Scott 2000).

2.1 Steel

For modelling the steel tube, two material models are used: the bilinear model with kinematic hardening and the Giuffre-Menegotto-Pinto model with isotropic strain hardening. It is concluded that models with the Giuffre-Menegotto-Pinto material with isotropic strain hardening show slightly better agreement with experimental results. Parameters needed to define the Giuffre-Menegotto-Pinto model are yield stress f_y, the initial modulus of elasticity E, strain-hardening ratio b (ratio between the post-yield tangent and initial modulus of elasticity) and parameters R_0, R_1, R_2 that define the shape and hysteretic behavior of this steel model. The values for f_y, E and b are usually obtained experimentally and available in advance. In tests where values for E and b were not reported, it is adopted that E=200GPa and b=0.01. The default values are used for parameters $R_0=15$, $R_1=0.925$ and $R_2=0.15$ (McKenna et al. 2000).

2.2 Concrete

For modelling concrete portion of a CFT column, the following material models are used: Kent-Scott-Park's model without and with tensile strength (concrete01 and concrete02), Popovic's model (concrete04) and Chang&Mander's model (concrete07). Among these material models, it is shown that the Chang and Mander's concrete model (Chang G.A. and Mander J.B. 1994) best describes the nonlinear behavior of CFT columns (Blagojević 2016). This concrete model with modifications has also been used by researchers (Tort and Hajjar 2009; Blagojevic, Kostic and Stosic 2017).
Parameters of the model are concrete compressive strength f_c, concrete strain at maximum compressive strength ε_{cc}, initial elastic modulus E_c, the tensile strength of concrete f_t, tensile strain at the maximum tensile strength of concrete ε_t and parameters that define the nonlinear branch of the model x_p, x_n and r. In order to determine the values of the model parameters for the confined concrete inside the steel tube that offer the best correlation with numerical results, several proposals are considered. The finally adopted relations are given with Equations 1 to 9. All parameters are functions of parameter C and the compressive strength f_c. In general, in reinforced concrete members, confinement effects are accounted for by increasing the peak compressive strength and the strain at peak compressive strength. Also, with confinement, the parameter x_n increases and the parameter r decreases. However, this increase in compressive strength, commonly, is not taken into account in rectangular CFT columns (Tomii M. and Sakino K. 1979a; Sakino et al. 2004). But, the confinement of the concrete core has a significant influence on the ductility of the concrete and needs to be considered (Tort and Hajjar 2009; Tomii M. and Sakino K. 1979a). The increase in ductility due to confinement is accounted for through the coefficient C in all concrete model parameters, except in the compressive strength parameter f_c. Parameters x_p and x_n are set to 2 and 30, respectively (McKenna, Frank, G. L. Fenves and M. H. Scott 2000).
The coefficient C is determined from equations proposed in papers by Mander, Priestley and Park. (1988) and Sakino et al. (2004). The effective lateral pressure σ_{re} is calculated from Equation 1 and the parameter C is calculated using Equation 2, where B and t are the width and the thickness of the steel tube, respectively, and σ_y is the yield stress of the steel tube:

$$\sigma_{re} = \frac{2 \cdot t^2 \cdot (B - t) \cdot \sigma_y}{(B - 2t)^3} \tag{1}$$

$$C = -1.254 + 2.254 \cdot \sqrt{1 + \frac{7.94 \cdot \sigma_{re}}{f_c}} - 2 \cdot \frac{\sigma_{re}}{f_c} \tag{2}$$

Other parameters of the concrete model are calculated from Equations 3-9 (Mark D. Denavit 2012):

$$\varepsilon_{c0} = \frac{(f_c[MPa] \cdot C)^{0.25}}{1150} \tag{3}$$

$$\varepsilon_{cc} = \varepsilon_{c0} \cdot (1 + 5 \cdot (C - 1)) \tag{4}$$

$$E_c = 8200 \cdot (f_c[MPa] \cdot C)^{0.375} \tag{5}$$

$$n = \frac{E_c \cdot \varepsilon_{cc}}{C \cdot f_c} \tag{6}$$

$$r = \frac{n}{n - 1} \tag{7}$$

$$f_t = 0.62 \cdot \sqrt{f_c[MPa]} \tag{8}$$

$$\varepsilon_t = \frac{2 \cdot f_t}{E_c} \tag{9}$$

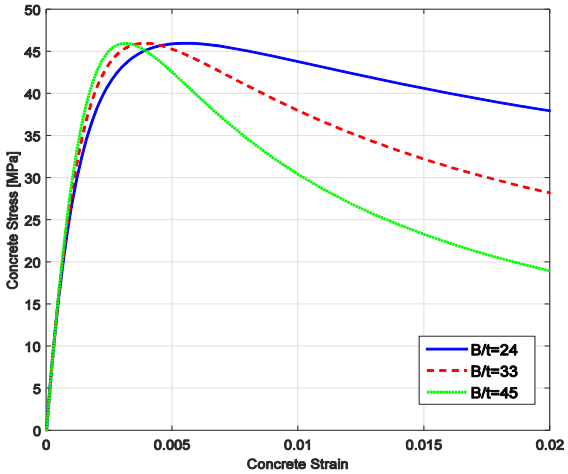

Figure 1. Concrete stress-strain model for different values of B/t

Figure 1 shows the stress-strain relations of the concrete model used in this study, for three different *B*/*t* ratios where *B* is the dimension of the steel tube and *t* is its thickness.

3. MODEL VALIDATION

The ability of the proposed model to accurately describe the nonlinear behavior of CFT columns is validated by comparing the results from the numerical model with the available experimental results. Experiments with different types of loading, types of structures, slenderness and *B*/*t* ratios are studied. Material nonlinearity is taken into account using nonlinear material models described in the previous section. Geometric nonlinearity is considered using the corotational formulation (Crisfield 1991). The same discretization of the CFT fiber section is used in all numerical simulations. The concrete portion of a square CFT section is discretized with 100 concrete fibers (10x10 division) and, for the discretization of the steel tube, 112 fibers are used (14x2 division per side). In tests with structures containing WF steel beams, a discretization with 108 fibers (12x3 fibers per flange and web), shown in

Figure 2, is used (Kostic and Filippou 2012). As mentioned before, the force based fiber beam-column element (Taucer F., Spacone E. and Fillippou F. 1991) is used with Gauss-Lobatto integration for integration over the element length.

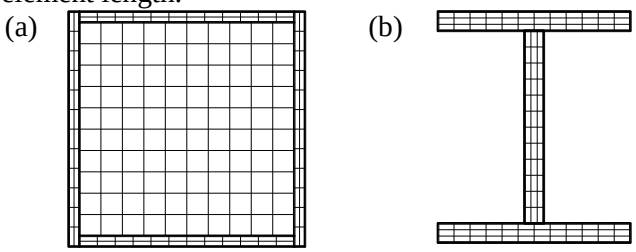

Figure 2: Section discretization of (a) square CFT column with 212 fibers (b) WF steel beam with 108 fibers

3.1 CFT column under proportional monotonic load

Among several experiments where CFT beam-column is subjected to proportional monotonic loading (Gourley et al. 2008), the experiments by Cederwall et al. (1991) and Bridge (1977) are selected in this study. A simply supported beam is exposed to an eccentric monotonically increasing axial force (Figure 3). Cederwall et al. (1991) considered the effect of high strength concrete on the inelastic response of a square CFT column subjected to uniaxial bending. From this group of tests, a total of 6 specimens, with varying concrete compressive strength, the thickness of the steel tube and yield stress of the steel tube, are numerically analyzed. Bridge investigated the effect of loading eccentricity, column slenderness and biaxial bending on nonlinear behavior of CFT columns. CFT column is modelled using two elements with three integration points. Table 1 contains data about geometry, material properties of the specimens and comparison between the experimental and numerical results. Specimen labels correspond to those of the original publication.

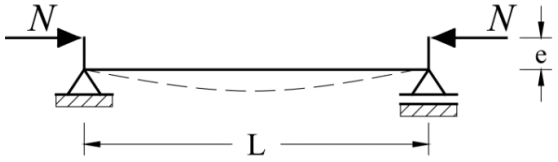

Figure 3: CFT beam-column test set-up

Table 1. Geometrical and material properties and analysis results for tests by Cederwall et al. (1991) and Bridge (1977)

Author	**Specimen**	**B x D x t (mm)**	**L (m)**	**α (deg)**	**e (mm)**	f'_c **[MPa]**	f_y **[MPa]**	$N_{u,num}/N_{u,exp}$
Cederwall et al.	1	120x120x5	3.00	0	20	47	304	0.99
(1991)	2	120x120x5	3.00	0	20	46	438	1.0
	6	120x120x8	3.00	0	20	46	300	0.98
	7	120x120x8	3.00	0	20	47	376	1.0
	9	120x120x8	3.00	0	20	103	379	1.02
	10	120x120x8	3.00	0	20	39	379	1.04
Bridge	SHC-1	203.7x203.9x9.96	2.13	0	38	30.2	291	1.07
(1977)	SHC-3	203.3x202.8x10.03	2.13	30	38	34.5	313	1.04
	SHC-4	202.8x203.4x9.88	2.13	45	38	33.1	317	1.05
	SHC-5	202.6x203.2x10.01	3.05	30	38	37.8	319	1.04
	SHC-6	203.2x202.1x9.78	3.05	45	64	32.1	317	1.03
	SHC-7	152.5x152.3x6.48	3.05	0	38	35.0	254	1.14
	SHC-8	152.5x152.3x6.48	3.05	0	64	35.0	254	1.19

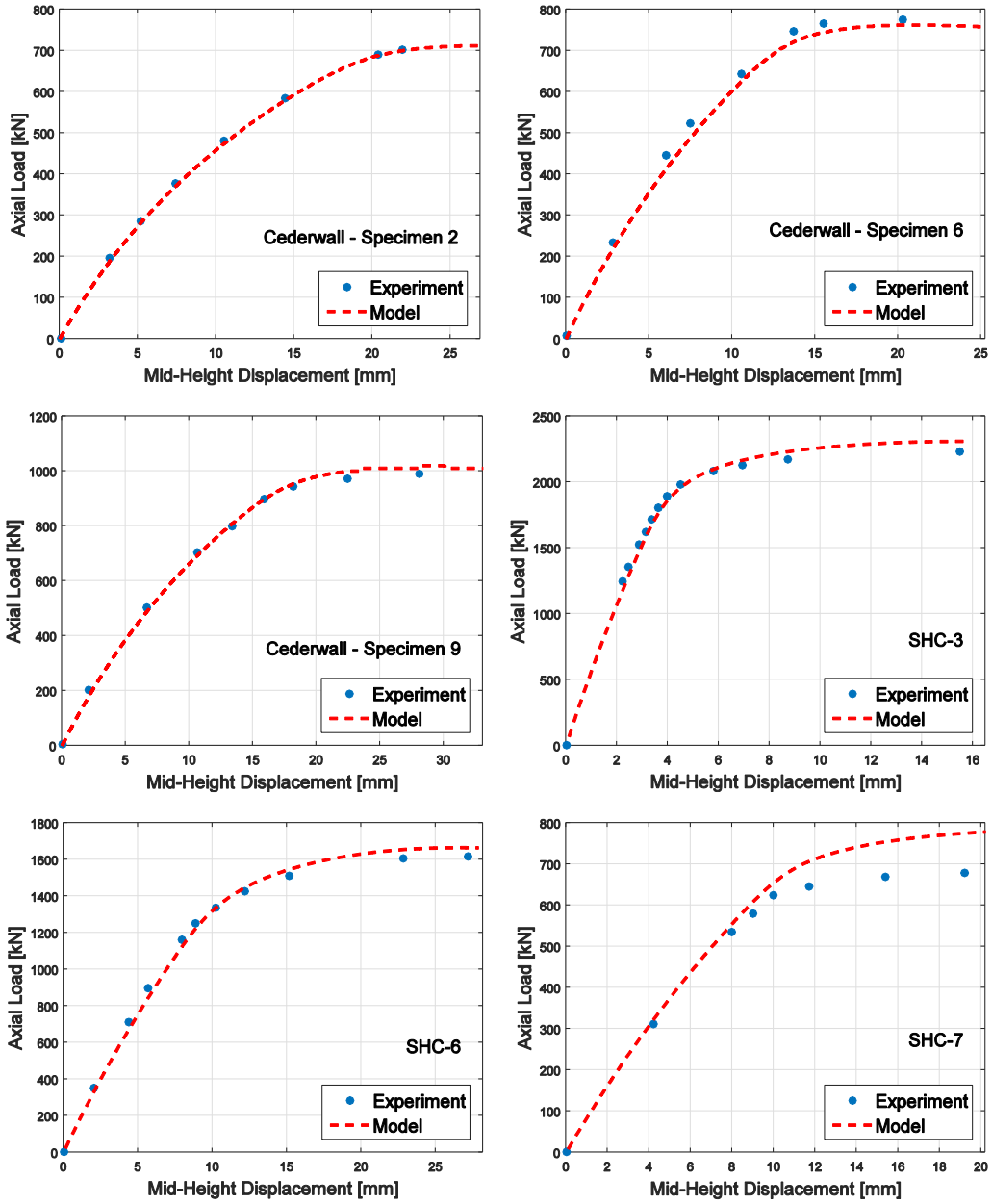

Figure 4: Axial load – Mid-height displacement relations for proportionally loaded CFT beam-columns

Figure 4 shows the comparison between the numerical and the experimental results for the relation between the axial load and the mid-height displacement for few tests, because of space limitations. Very good agreement between the numerical and experimental results can be observed for all specimens tested by Cederwall et al. Also, the numerical model managed to properly simulate tests done by Bridge. The largest differences, noticed in tests SHC-7 and SHC-8, correspond to the specimens with the highest slenderness and the lowest steel grade. These errors can be explained by the model limitation since it does not consider the local buckling of the steel tube.

3.2 CFT column under non-proportional monotonic load

Tomii and Sakino (1979b) conducted experiments on CFT columns under constant axial force and increasing uniaxial bending moment (Figure 5). One element with five integration points is used to model the CFT column. Table 2 contains information regarding the analyzed specimens and the numerical results. The moment-rotation relations for four selected tests are shown in Figure 6.

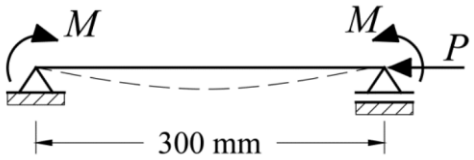

Figure 5. Tomii and Sakino (1979b) experiment set-up

Table 2. Geometrical and material properties and analysis results of tests by Tomii and Sakino (1979b)

Specimen	B x t (mm)	$f'c$ [MPa]	fy [MPa]	N/N_0	$M_{u,num}/M_{u,exp}$
II-2	100x2.27	25.9	339	0.18	1.05
II-3	100x2.20	25.9	339	0.26	1.03
II-5	100x2.22	25.9	289	0.48	0.94
II-6	100x2.22	25.9	289	0.57	0.89
IV-3	100x4.25	22.4	288	0.29	1.01
IV-5	100x4.25	23.8	285	0.48	1.02
IV-6	100x4.26	23.8	288	0.57	1.02

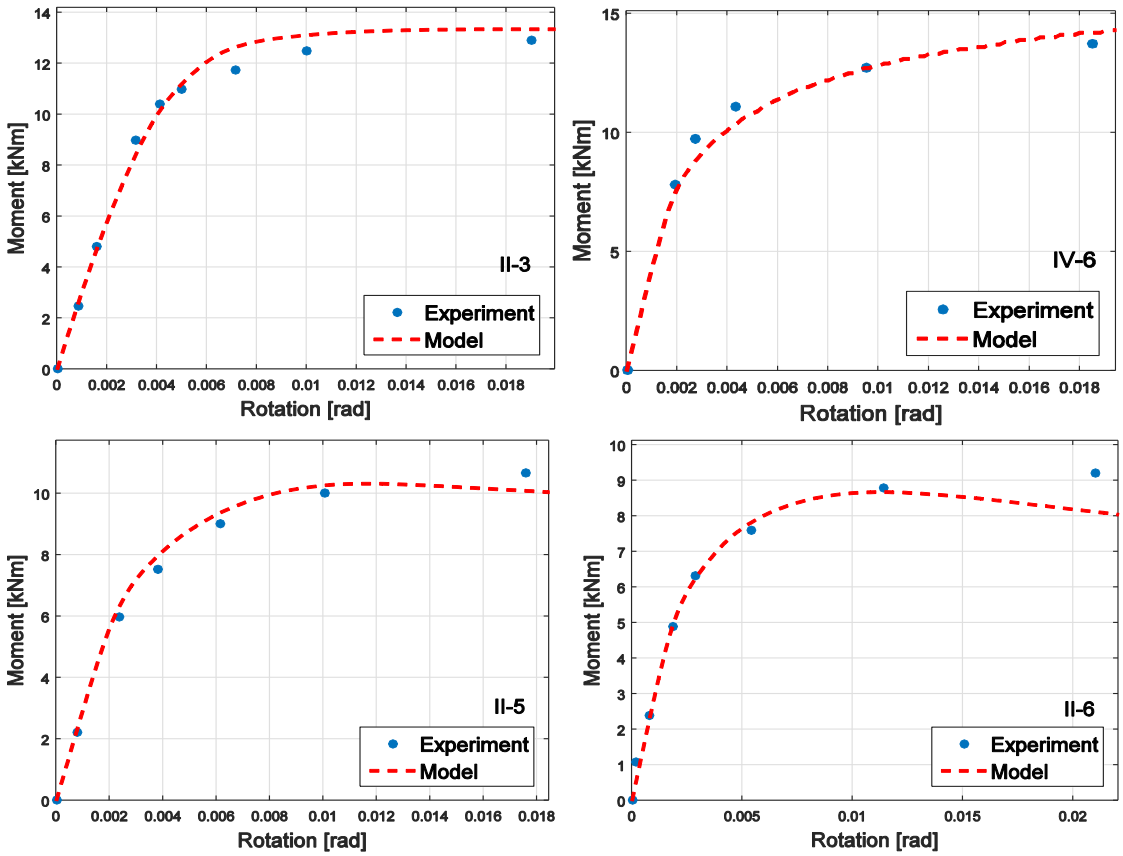

Figure 6. Moment-Rotation relations for non-proportionally loaded CFT beam-columns

Comparing the numerical and the experimental results, it can be concluded that for specimens with B/t ratio equal to 24, there is a good agreement for all levels of axial load. However, for specimens II-5 and II-6, with B/t equal to 45 and axial load levels higher than 0.48, the model is slightly less accurate. This can be attributed to the underestimation of the confinement effects. For tests with B/t equal to 45 and axial load levels smaller than 0.48, numerical results agree very well with the experimental results.

3.3 CFT column under cyclic loading

Sakino and Tomii (1981) experimentally tested square CFT columns subjected to the cyclic lateral displacements under constant axial force (Figure 7). The effect of varying B/t ratio and axial load level on the cyclic behavior of CFT columns is investigated. Two elements, with three integration points per element, are used to model the CFT column. Table 3 summarizes the geometrical and material properties of the tested specimens.

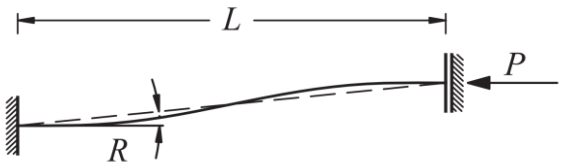

Figure 7. CFT beam-column exposed to cyclic loading

Table 3. Geometrical and material properties for CFT columns under cyclic loading

Specimen	B x t (mm)	*f'c* [MPa]	*fy* [MPa]	N/N_0
CIIS3-2	100x2.17	22.26	295.18	0.18
CIIS3-3	100x2.17	22.26	295.18	0.29
CIIIS3-2	100x2.96	22.45	293.21	0.19
CIIIS3-3	100x2.96	22.45	293.21	0.28
CIVS3-2	100x4.21	20.36	290.27	0.19
CIVS3-3	100x4.21	20.36	290.27	0.28
CIVS3-5	100x4.21	20.36	290.27	0.47

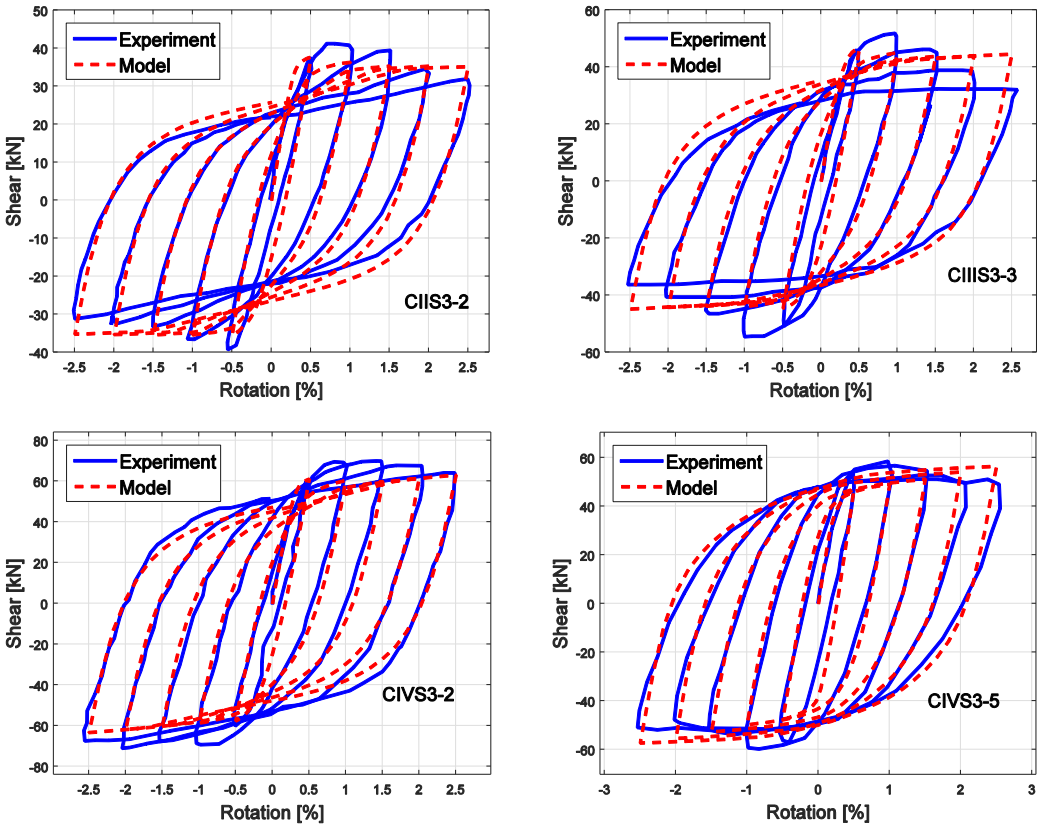

Figure 8. Cyclic loading: Shear-Rotation relations

Because of space limitations, just four test results are shown in Figure 8. In general, the proposed numerical model accurately simulated the cyclic behavior of CFT columns: initial and unloading stiffness and gradual stiffness reduction. The agreement with the experimental results is the best for samples with B/t ratio equal to 25 irrespective of the level of axial force. For higher B/t ratios, the agreement is better for the levels of axial force below 0.3 since for higher levels of axial force there is significant cyclic strength degradation due to the local buckling of the steel tubes (Hajjar, Molodan, and Schiller 1998) which is not taken into account by the model.

3.4 Beam-Column structural subassembly

The behavior of a structural subassembly consisting of CFT column and WF steel beams was the subject of the experimental study by Kawaguchi and Morino (2001). Among several types of tested subassemblies, the interior column type is analyzed in this paper. Experiment set-up together with the proposed numerical model is shown in Figure 9. CFT columns and short WF steel beams are modelled using one element with five integration points over element length, while longer WF steel beams are modelled with two elements with three integration points over the element length because the displacement of the mid-length node is monitored. Since the steel hardening ratio *b* was not reported, the value of 2% is adopted. Modelling of the connections is not part of this study, therefore, only specimens with CFT column yielding are considered.

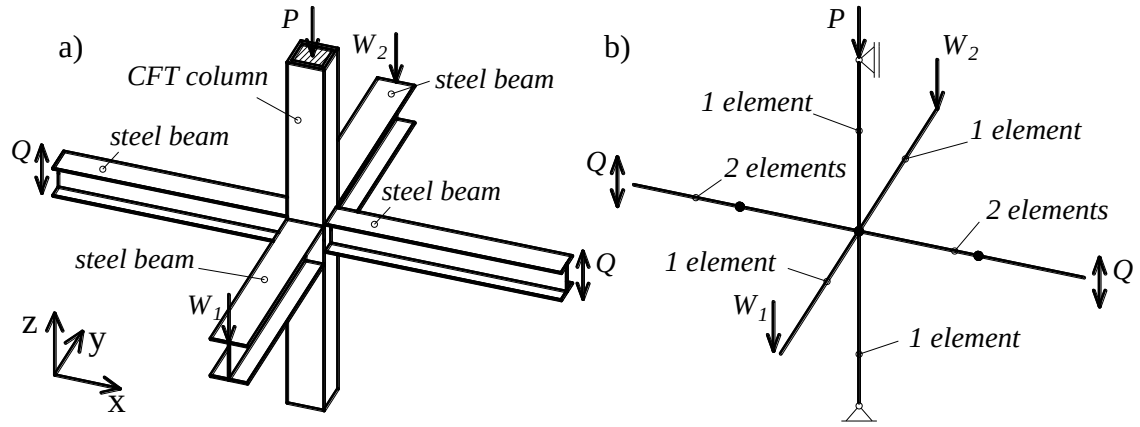

Figure 9. Beam-column structural subassembly test set-up (a) and numerical model (b)

The long-term loading is simulated with a constant axial force P and constant vertical loads (W1, W2) applied to the CFT column and to the ends of the shorter beams (Figure 9). The earthquake loading is simulated with a pair of anti-symmetric, alternately repeating vertical forces Q applied to the ends of the longer beams. Dimensions of CFT columns are 125x125x5.74mm. Properties of WF beams can be found elsewhere (Kawaguchi Jan and Morino Shosuke 2001).

Table 4. Material properties and vertical load values for Kawaguchi and Morino tests (2001)

Specimen	***fc* [MPa]**	***fy,CFT* [MPa]**	***fy,BEAM* [MPa]**	**W1,W2 [kN]**
I-15C00	19.28	394.9	400	0,0
I-15C11	19.51	394.9	400	9.8,9.8
I-15C20	20.04	394.9	400	21.0,0
I-15C31	19.82	394.9	400	31.0,9.8

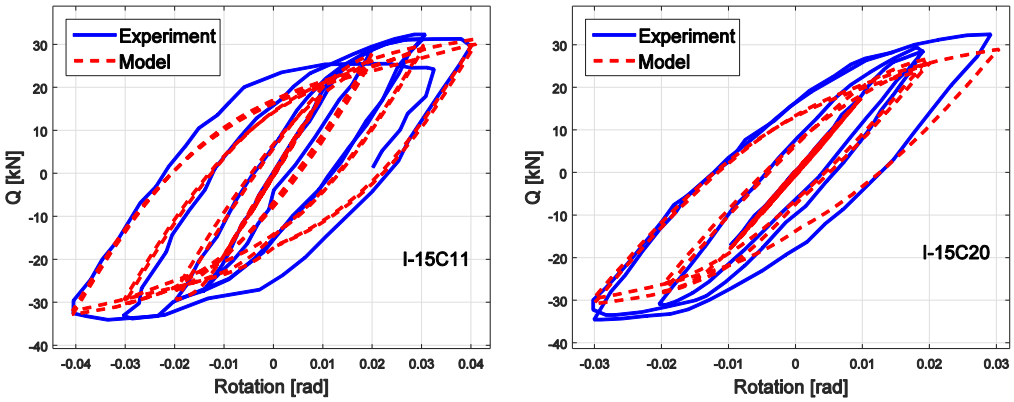

Figure 10. Force-rotation relation for the beam-column structural subassembly

Figure 10 shows typical results obtained for this group of tests. A good agreement referring to the initial stiffness and the ultimate strength is obtained. It is assumed that better correlation with the experimental results would be achieved considering the rigidity of the beam/column connections.

3.5 Dynamic analysis of a plane frame

Finally, the last numerically analyzed example refers to the non-linear time history analysis of a multi-story plane frame consisting of CFT columns experimentally tested by Herrera et al. (2004). The test structure was a scaled model of a prototype MRF extracted from the four-story building. Test structure was exposed to different levels of seismic hazards using the pseudo-dynamic testing method. The numerical model used in this paper is shown in Figure 11. Steel beams are modelled using one element with five integration points, while CFT columns are modelled with two elements and three integration points per element. Leaning columns are modelled as elastic beam-column elements with section properties defined as the sum of the section properties of one-half of interior columns in a story of the prototype building. The mass is lumped to the nodes of the leaning columns, at story heights. Loading beams are modelled as axially rigid truss elements. Loading beams and leaning columns are connected using zero-length rotational spring elements with very small stiffness values. To ensure that the horizontal displacements of all the nodes on one floor are the same, *equalDOF* command is used. In order to account for the stiffness of the beam-to-column connections, rigid joint offset command is applied to the ends of the beams and columns. Damping is taken into account as Rayleigh damping. The mass proportional damping is assigned to the nodes of the leaning column (where masses are concentrated). The stiffness proportional damping is assigned to the members with realistic values of stiffness, i.e. frame beams and columns apart from the leaning column and the loading beams (Charney 2008). The mass proportional damping factor is 0.15451 and the stiffness proportional damping factor is 0.001176 (Herrera et al. 2004). The Newmark-Beta (γ=0.5, β=0.25) time integration method is used. Details regarding the geometry and material properties of structural elements can be found elsewhere (Herrera et al. 2004). For the proposed numerical model, a good agreement between the calculated and the reported first three natural periods is obtained (Table 5).
The model is firstly subjected to the acceleration record of the Northridge Canoga Park (1994) scaled to the DBE (Design Basis Earthquake) hazard level. Before exposing the model to the same acceleration record but scaled to the MCE (Maximum Considered Earthquake) hazard level, the structure is calmed. The final time-displacement relation for the MCE hazard level is obtained by subtracting the residual displacement after the DBE hazard level.

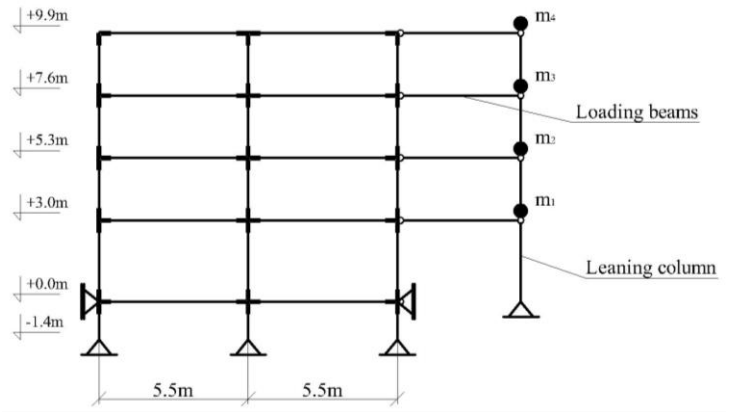

Figure 11. Numerical model of the test structure (Herrera et al. 2004)

Table 5. The first three natural periods for the frame structure

Period	T_1[s]	T_2[s]	T_3[s]
Experiment	1.21	0.37	0.20
Model	1.07	0.36	0.16

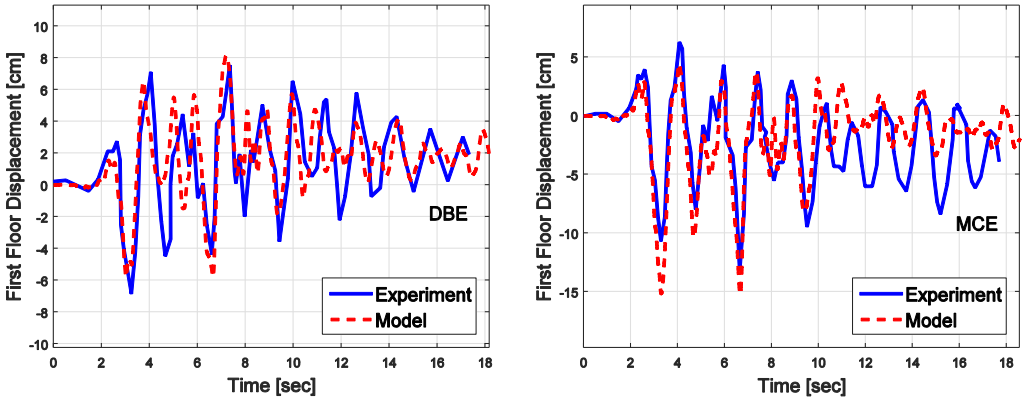

Figure 12. First floor displacement - time history results for DBE and MCE hazard levels

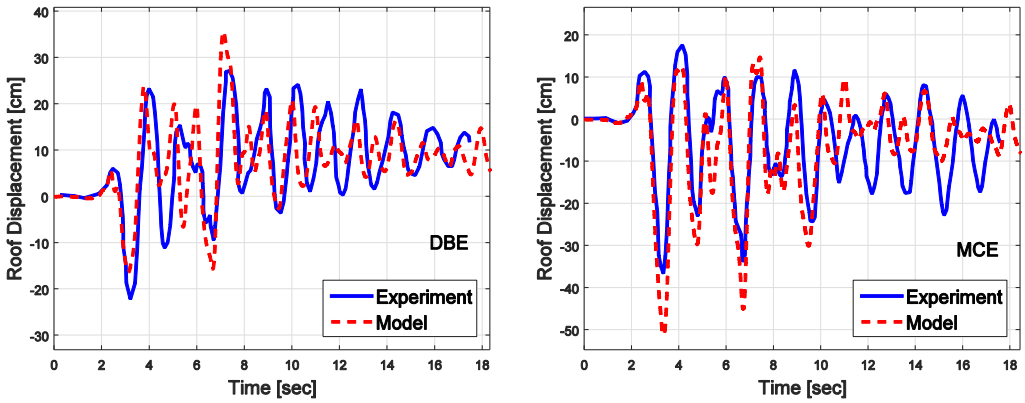

Figure 13. Roof displacement – time history results for DBE and MCE hazard levels

Figures 12 and 13 show the first floor and the roof displacement history for two analyzed earthquake records. As can be seen, the numerically obtained displacements follow well the experimental results. In this example, under both levels of the earthquake, yielding and local buckling of steel beams are noticed while CFT columns experienced inelastic deformations due to concrete cracking and crushing and yielding of steel tube (Tort and Hajjar 2009).

4. CONCLUSIONS

The paper presents the results of the study regarding the nonlinear analysis of square CFT columns using the distributed plasticity fiber beam/column element. The commonly available numerical models for the uniaxial constitutive relations for steel and concrete are used and evaluated. The parameters of the used models that approximate best the behavior of CFT columns under static loading conditions are determined. This numerical model is then validated through a number of tests with available experimental results. These tests include different types of loading (cyclic static and dynamic), types of structures (one column tests, beam-column structural subassembly, 2D frame example) with different slenderness of tested specimens and B/t ratio. In general, the proposed numerical model shows a high level of accuracy for practical application. However, for slender specimens (B/t ratio higher than 45) and lower grades of steel that are prone to local buckling, it is advised to use numerical models that take into account these effects.

5. ACKNOWLEDGEMENTS

Authors thank the Ministry of Science of the Republic of Serbia for financial support under project number III 42012.

6. REFERENCES

Blagojević Nikola. (2016). Nonlinear Analysis of Frames with CFT Columns. *Faculty of Civil Engineering, Belgrade*, MSc Thesis.

Blagojevic Nikola, Svetlana Kostic and Sasa Stosic. (2017). Fiber Finite Element in Nonlinear Analysis of Square CFT Columns. *Gradjevinski Materijali i Konstrukcije* 60 (1):31–46.

Bridge R. Q. (1977). Concrete Filled Steel Tubular Columns.

Cederwall K., Engstrom B. and Grauers M. (1991). High-Strength Concrete Used in Composite Columns. *2nd Int Symp on Utillization of High-Strength Concrete. American Concrete Institute (ACI)*, 195–214.

Chang G.A. and Mander J.B. (1994). Seismic Energy Based Fatigue Damage Analysis of Bride Columns. *NCEER* 94-0006 (March).

Charney, Finley A. (2008). Unintended Consequences of Modeling Damping in Structures. *Journal of Structural Engineering* 134 (4):581–592.

Crisfield, M. A. (1991). *Non-Linear Finite Element Analysis of Solids and Structures*. Chichester ; New York: Wiley.

Denavit, M. D., J. F. Hajjar and R. T. Leon. (2012). Stability Analysis and Design of Steel-Concrete Composite Columns. In *Proceedings of the Annual Stability Conference, Structural Stability Research Council, Grapevine, Texas, April*, 18–21.

Denavit, Mark D. (2012). *Characterization of Behavior of Steel-Concrete Composite Members and Frames with Applications for Design*. University of Illinois at Urbana-Champaign.

Gourley, Brett C., Cenk Tort, Mark D. Denavit, Paul H. Schiller and Jerome F. Hajjar. (2008). A Synopsis of Studies of the Monotonic and Cyclic Behavior of Concrete-Filled Steel Tube Members, Connections, and Frames. Newmark Structural Engineering Laboratory. University of Illinois at Urbana-Champaign.

Hajjar, Jerome F., Aleksandr Molodan and Paul H. Schiller. (1998). A Distributed Plasticity Model for Cyclic Analysis of Concrete-Filled Steel Tube Beam-Columns and Composite Frames. *Engineering Structures* 20 (4–6):398–412.

HERRERA, Ricardo, Brian LEWIS, James RICLES, and Richard SAUSE. (2004). EXPERIMENTAL STUDIES ON STEEL MOMENT RESISTING FRAMES WITH CONCRETE FILLED TUBE COLUMNS UNDER EARTHQUAKE LOADING CONDITIONS.

Kawaguchi Jan and Morino Shosuke. (2001). Experimental Study on Elasto-Plastic Behavior of Three-Dimensional Frames Consisting of CFT Columns. *J. Struct. Constr. Eng*, no. No. 541 (March):187–95.

Kostic, Svetlana M. and Filip C. Filippou. (2012). Section Discretization of Fiber Beam-Column Elements for Cyclic Inelastic Response. *Journal of Structural Engineering* 138 (5):592–601.

Mander J.B., Priestley J.N. and Park R. (1988). Theoretical Stress-Strain Model for Confined Concrete.

McKenna, Frank, G. L. Fenves and M. H. Scott. (2000). Open System for Earthquake Engineering Simulation. *University of California, Berkeley, CA*.

Portolés, J.M., M.L. Romero, F.C. Filippou and J.L. Bonet. (2011). Simulation and Design Recommendations of Eccentrically Loaded Slender Concrete-Filled Tubular Columns. *Engineering Structures* 33 (5):1576–93.

Sakino K. and Tomii M. (1981). Hysteretic Behavior of Concrete Filled Square Steel Tubular Beam-Columns Failed in Flexure. Trans Jpn Concr Inst.

Sakino, Kenji, Hiroyuki Nakahara, Shosuke Morino and Isao Nishiyama. (2004). Behavior of Centrally Loaded Concrete-Filled Steel-Tube Short Columns. *Journal of Structural Engineering* 130 (2):180–188.

Taucer F, Spacone E and Fillippou F. (1991). A Fiber Beam-Column Element For Seismic Response Analysis of Reinforced Concrete Structures. *Earthquake Engineering Research Centar, University of California Berkley*, no. Report No. UCB/EERC-91/17.

Tomii M. and Sakino K. (1979a). Elasto-Plastic Behavior of Concrete Filled Square Steel Tubular Beam-Columns. *Trans Architec Inst Jpn*, no. 111–22.

Tomii M. and Sakino K. (1979b). Experimental Studies on the Ultimate Moment of Concrete Filled Square Steel Tubular Beam-Columns.

Tort, Cenk and Jerome F. Hajjar. (2009). Mixed Finite-Element Modeling of Rectangular Concrete-Filled Steel Tube Members and Frames under Static and Dynamic Loads. *Journal of Structural Engineering* 136 (6):654–664.

Valipour, Hamid R. and Stephen J. Foster. (2010). Nonlinear Static and Cyclic Analysis of Concrete-Filled Steel Columns. *Journal of Constructional Steel Research* 66 (6):793–802.

Varma, Amit H., Richard Sause, James M. Ricles and Qinggang Li. (2005). Development and Validation of Fiber Model for High-Strength Square Concrete-Filled Steel Tube Beam-Columns. *ACI Structural Journal* 102 (1):73.